Journal of Photonic Materials and Technology
2026, Vol. 11, No. 2, pp. 23–32
https://doi.org/10.11648/j.jpmt.20261102.11

Research Article

Development and Experimental Evaluation of WO_3-Doped Boro-Tellurite Glasses as Transparent Lead-Free X-ray Shielding Materials

Shihabudheen VT, Ghizal Firdous Ansari*

Physics Department, Madhyanchal Professional University, Bhopal, India

Abstract

The development of environmentally friendly radiation shielding materials has gained considerable attention as an alternative to toxic lead-based shields used in medical and industrial applications. In the present study, a series of WO_3-doped boro-tellurite glasses with the composition (55−x) TeO_2-20B_2O_3-15ZnO-10Na_2CO_3-xWO_3 (where x = 5, 10, 15, and 20 mol%) were successfully synthesized using the conventional melt-quenching technique. The X-ray shielding performance of the prepared glass samples (TBZNW1-TBZNW4) was experimentally evaluated using an Ultisys 52 diagnostic X-ray system operated over the tube voltage range of 50-140 kVp. The shielding characteristics were assessed in terms of the linear attenuation coefficient (LAC), mass attenuation coefficient (MAC), half-value layer (HVL), tenth-value layer (TVL), mean free path (MFP), radiation attenuation efficiency (Att%), and lead equivalent thickness (LET). The results revealed that increasing the WO_3 concentration significantly enhanced the attenuation capability of the glass system owing to the increase in density and effective atomic number. The TBZNW4 glass, containing 20 mol% WO_3, exhibited the highest LAC and MAC values together with the lowest HVL, TVL, and MFP, indicating superior X-ray shielding performance. Moreover, the attenuation efficiency increased with WO_3 content, while the lead equivalent thickness demonstrated the potential of the developed glasses to replace conventional lead-based shielding in diagnostic energy ranges. Comparison with previously reported shielding materials further confirmed the improved attenuation performance of the present glass system. These findings demonstrate that WO_3-doped boro-tellurite glasses are promising, environmentally benign candidates for transparent radiation shielding applications in medical diagnostic facilities, laboratories, and other radiation environments.

Keywords

Boro-tellurite Glass, WO_3, X-ray Shielding, Radiation Attenuation, Linear Attenuation Coefficient, Lead-free Shielding Materials, Heavy Metal Oxide, Diagnostic X-rays

1. Introduction

The widespread adoption of radiation-based technologies has significantly increased human exposure to ionizing radiation over the past few decades. X-rays and γ-rays are now indispensable in numerous fields, including medical diagnostics,

*Correspondence: Ghizal Firdous Ansari (ansarigf@rediffmail.com)

Received: 3 August 2026; **Accepted:** 11 August 2026; **Published:** 27 August 2026

industrial inspection, agriculture, scientific research, and nuclear energy applications [1, 2]. Despite their numerous benefits, prolonged or uncontrolled exposure to ionizing radiation can have serious biological consequences, such as cellular damage, genetic mutations, radiation sickness, and an increased risk of cancer [3, 4]. Consequently, ensuring effective radiation protection has become a critical requirement for safeguarding both human health and the environment [5]. To minimize radiation-associated risks, the National Council on Radiation Protection and Measurements (NCRP) introduced the ALARA (As Low As Reasonably Achievable) principle, which emphasizes maintaining radiation exposure at the lowest practical level without compromising the intended application [6-8]. In general, radiation protection can be achieved through three fundamental approaches: reducing exposure time, increasing the distance from the radiation source, and employing suitable shielding materials [9]. Although limiting exposure time and maintaining safe distances are effective in many situations, these strategies are often impractical for personnel who routinely work with radiation sources in hospitals, research laboratories, and industrial facilities. Consequently, the use of shielding materials remains the most reliable and widely adopted method for minimizing radiation exposure. The International Commission on Radiological Protection (ICRP) also recognizes shielding as one of the primary measures for ensuring radiation safety [10]. The effectiveness of a shielding material largely depends on its ability to attenuate incoming radiation, which is strongly influenced by its density and atomic number. Materials possessing high density and high atomic-number elements generally exhibit superior photon attenuation because they provide a greater probability of photon interaction and energy absorption [11]. For several decades, lead and lead-based materials have been the preferred choice for radiation shielding owing to their excellent attenuation capability, low cost, and widespread availability [12-14]. However, the high toxicity of lead has become a major concern due to its detrimental effects on both human health and the environment. Long-term exposure to lead has been associated with neurological disorders, kidney dysfunction, cardiovascular diseases, and developmental abnormalities. Owing to these hazards, the United States Environmental Protection Agency (USEPA) classifies lead among the most hazardous toxic substances [15, 16]. These concerns have accelerated global efforts to develop environmentally benign, lead-free shielding materials that can provide comparable or superior radiation protection without the associated health risks [5]. Among the proposed alternatives, heavy metal oxides (HMOs) have attracted considerable attention because they combine high density and large atomic numbers with relatively low toxicity compared with conventional lead-based materials. Incorporating HMOs into shielding materials can significantly enhance photon attenuation while maintaining environmental compatibility [17-19]. In addition to radiation shielding efficiency, the selection of suitable shielding materials also requires consideration of several practical factors, including mechanical strength, chemical durability, thermal stability, optical transparency, ease of fabrication, and long-term environmental sustainability [19].

In recent years, considerable research has been devoted to the development of lead-free materials for radiation shielding. A variety of materials, including polymers, concretes, ceramics, alloys, composites, and glasses, have been investigated as environmentally friendly alternatives to conventional lead-based shields [20, 21]. Among these candidates, glass has emerged as one of the most promising materials because it combines excellent transparency with good chemical durability, ease of fabrication, relatively low production cost, and effective attenuation of ionizing radiation [22, 23]. These advantages make glass particularly attractive for applications requiring both radiation protection and optical visibility, such as diagnostic viewing windows, protective barriers, and laboratory shielding panels. The radiation shielding capability of glass can be further enhanced by incorporating heavy metal oxides (HMOs) into the glass network. Such modifications increase the density and effective atomic number of the material, thereby improving its ability to absorb and scatter high-energy photons [24, 25]. In addition to enhancing shielding performance, HMO incorporation allows the physical, structural, and optical properties of glass to be tailored according to the requirements of specific applications.

Among the different glass families, boro-tellurite glasses have attracted considerable interest because of their excellent combination of optical, thermal, and radiation shielding characteristics. Boron oxide (B_2O_3) is a well-established glass former that contributes high transparency, low melting temperature, and favourable optical properties, making it an important constituent in advanced glass systems [26]. Tellurium dioxide (TeO_2), another important glass former, is distinguished by its high refractive index, relatively high density, excellent chemical stability, and resistance to moisture and corrosion [20, 25]. Owing to the high atomic number of tellurium, TeO_2-containing glasses exhibit enhanced interactions with X-rays and γ-rays, resulting in improved attenuation efficiency compared with many conventional oxide glasses [27]. Consequently, combining B_2O_3 and TeO_2 provides a versatile glass matrix capable of delivering both desirable physical properties and effective radiation shielding performance [28].

In the present glass system, ZnO and Na_2CO_3 serve as network modifiers that improve the overall characteristics of the glass. ZnO enhances glass formation while reducing the melting temperature, thereby facilitating the fabrication process Na_2CO_3 on the other hand, contributes to improved chemical durability, mechanical strength, and water resistance, resulting in a more stable glass network [26, 29]. Previous investigations have consistently demonstrated that boro-tellurite glasses containing heavy metal oxides exhibit excellent attenuation characteristics against both X-rays and γ-rays, making them promising candidates for radiation shielding applications [25]. Among the various heavy metal oxides, tungsten trioxide (WO_3) has emerged as one of the most effective and environmentally acceptable additives for radiation shielding glasses [30]. The high atomic number and density of tungsten significantly increase the probability of photon interaction, thereby improving the attenuation of ionizing radiation without introducing the toxicity associated with lead [31]. Incorporating WO_3 into the glass matrix not only enhances photon absorption and scattering but also increases the density of the glass, leading to improved shielding efficiency [32]. In addition, WO_3 is inexpensive, chemically stable, and environmentally benign, making it highly suitable for the development of sustainable lead-free shielding materials [33, 34]. Beyond its contribution to radiation attenuation, WO_3 also improves several important material properties. Previous studies have shown that the incorporation of WO_3 enhances the structural integrity, optical behaviour, chemical durability, and resistance to crystallization of tellurite-based glasses [27, 35, 36]. The simultaneous improvement in both functional and shielding properties makes WO_3 an attractive substitute for toxic lead in advanced radiation shielding glass systems [21].

2. Materials and Methodology

The glass samples were synthesized using analytical-grade raw materials procured from Otto Chemie. The precursor chemicals included tellurium dioxide (TeO_2, ≥99%), zinc oxide (ZnO, 99%), boron trioxide (B_2O_3, 97%), tungsten (VI) oxide (WO_3, 99.9%), and reagent-grade sodium carbonate (Na_2CO_3). The glass compositions were prepared according to the formula (55 − x) TeO_2-$20B_2O_3$-15ZnO-$10Na_2CO_3$-xWO_3, where the WO_3 concentration (x) was varied as 5, 10, 15, and 20 mol%. Accordingly, the prepared glass samples were designated as TBZNW1, TBZNW2, TBZNW3, and TBZNW4, corresponding to 5, 10, 15, and 20 mol% WO_3, respectively. A conventional melt-quenching technique was employed to fabricate the glass samples. Initially, the required quantities of each precursor were accurately weighed using a high-precision electronic balance and thoroughly mixed to obtain homogeneous batches. The mixed powders were transferred into an alumina crucible and heated in a muffle furnace for approximately 90-100 min. Complete melting of the batch occurred at around 900°C. To improve melt homogeneity, the crucible was briefly removed, manually swirled, and then returned to the furnace until the temperature reached 960°C. The molten glass was subsequently poured into a preheated stainless-steel mould. To relieve the residual thermal stresses developed during quenching, the cast samples were immediately transferred to another muffle furnace and annealed at 300°C for 3h. Finally, the samples were allowed to cool gradually to room temperature. The resulting products were transparent, pellet-shaped glass specimens with an approximate thickness of 3 mm and a diameter of 14 mm.

3. Result and Analysis

3.1. X-Ray Shielding Analysis

The X-ray shielding performance of the TBZNW1-TBZNW4 glass samples was evaluated using an Ultisys 52 diagnostic X-ray unit operated at a tube current of 10 mA and tube voltages ranging from 50 to 140 kVp. The shielding characteristics of the synthesized lead-free glass system were determined using Beer-Lambert's law, which describes the attenuation of X-ray photons as they pass through a shielding material. The relationship is expressed as follows [37]:

$$I = I_0\, e^{(-\mu x)} \tag{1}$$

where (I_0) and (I) denote the incident and transmitted photon intensities, respectively, while (μ) and (x) represent the linear attenuation coefficient (LAC) and the thickness of the glass sample. Based on this relationship, several important shielding parameters, including the linear attenuation coefficient (LAC), mass attenuation coefficient (MAC), half-value layer (HVL), tenth-value layer (TVL), mean free path (MFP), attenuation efficiency (Att%), and lead equivalent thickness (LET), were determined and discussed in the subsequent sections. The linear attenuation coefficient (LAC) represents the attenuation capability of a material per unit thickness and depends on photon energy, density, atomic number, and sample thickness. The LAC values were calculated from the measured incident and transmitted X-ray intensities using Beer-Lambert's equation. The mass attenuation coefficient (MAC) was subsequently obtained by normalizing the LAC with the density of each glass sample using Eq. (1) [38]. Higher values of both LAC and MAC indicate superior X-ray shielding performance [37].

3.2. Linear Attenuation Coefficient (LAC) and Mass Attenuation Coefficient (MAC)

The linear attenuation coefficient (LAC, μ) is a key parameter used to assess the X-ray shielding capability of a material, as it represents the attenuation of X-ray intensity per unit thickness. Its value depends on several factors, including photon energy, density, atomic number, and sample thickness. In this study, the LAC values for the TBZNW1-TBZNW4 glass samples were determined using Beer-Lambert's law based on the measured incident and transmitted X-ray intensities. The mass attenuation coefficient (MAC) was then calculated by dividing the LAC by the density of each sample according to Eq. (1) [38].

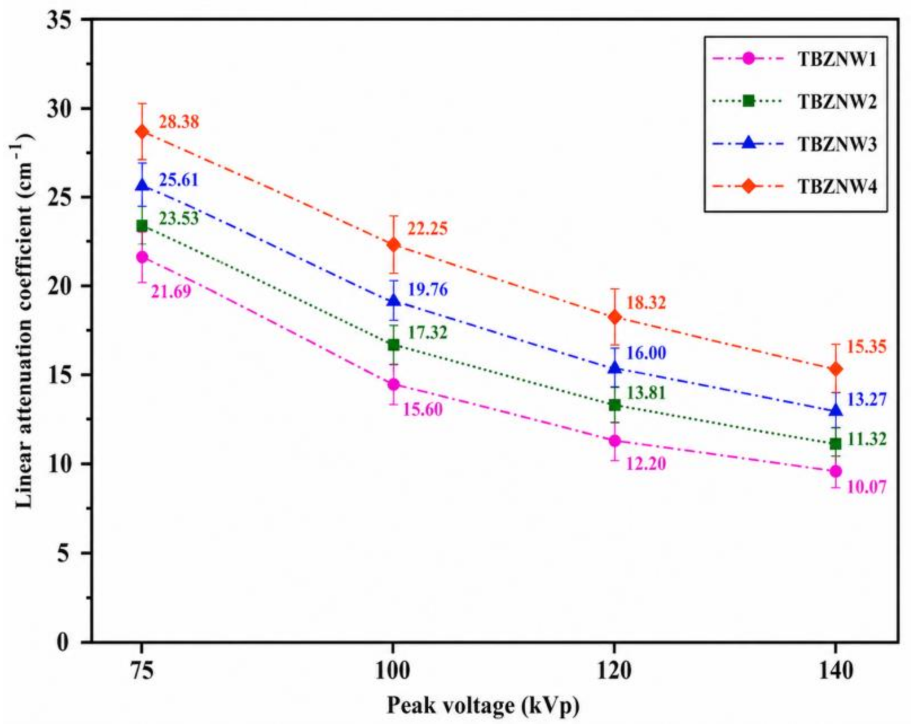

Figure 1. *Linear attenuation coefficient (LAC) Vs Peak Voltage.*

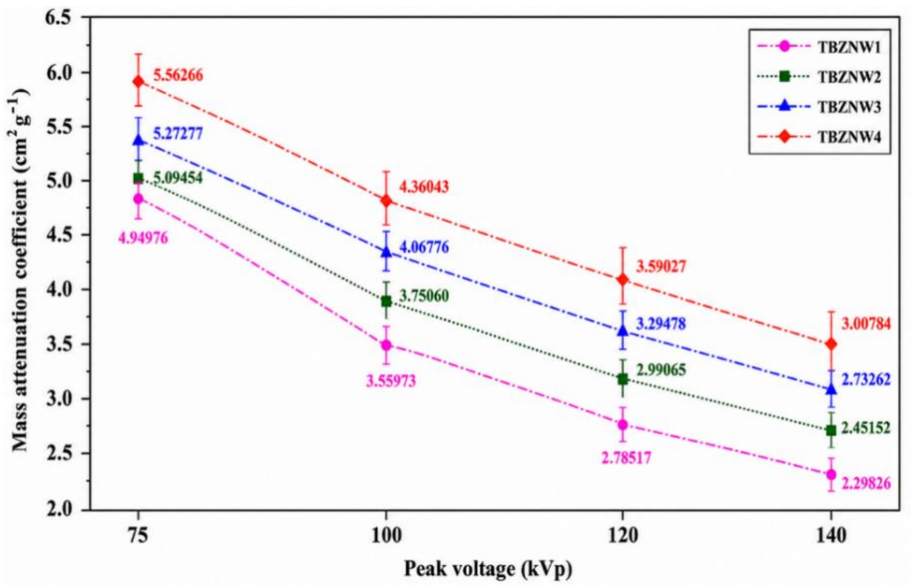

Figure 2. *Mass attenuation coefficient (MAC) Vs X-ray tube voltage.*

The MAC reflects the probability of photon interaction per unit mass and provides an intrinsic measure of the shielding efficiency of the material. Generally, higher LAC and MAC values correspond to better radiation attenuation performance [37].

$$MAC = \mu/\rho \ (cm^2/g) \quad (2)$$

The variation of LAC and MAC with X-ray tube voltage for the TBZNW1-TBZNW4 glass samples is presented in Figure 1 & 2, while the corresponding numerical values are listed in Table 1. The results show that both attenuation coefficients are relatively high at lower X-ray tube voltages and gradually decrease with increasing tube voltage. This behaviour is attributed to the higher penetration capability of high-energy X-ray photons, which reduces their interaction probability within the glass matrix, thereby lowering the attenuation coefficients [39, 40].

An increase in WO_3 concentration from TBZNW1 to TBZNW4 resulted in a noticeable enhancement in both LAC and MAC values [35, 41]. This improvement is primarily associated with the increase in density and effective atomic weight caused by the incorporation of tungsten oxide into the glass network. As the density increases, the probability of photon absorption and scattering also increases, leading to improved radiation attenuation. Consequently, TBZNW4, containing the highest WO_3 concentration, exhibited the greatest attenuation capability among all the investigated samples.

Furthermore, the developed TBZNW glass system exhibited higher LAC values than commercial window glass and commercial lead glass [42]. The obtained attenuation coefficients were also superior to those reported for several lead-free glass systems, including Gd_2O_3-based glasses [40], BaO-based glasses [42], and CeO_2-doped glasses [43]. Likewise, the MAC values exceeded those reported for conventional lead-containing shielding materials such as lead-borate glasses [44] and lead-based polymer composites [45]. These findings confirm that increasing the WO_3 content significantly enhances the radiation shielding performance of the TBZNW glass system, demonstrating its strong potential as an environmentally friendly lead-free shielding material for medical diagnostic applications.

3.3. Half-Value Layer (HVL) and Tenth-Value Layer (TVL)

The half-value layer (HVL) and tenth-value layer (TVL) are important shielding parameters used to evaluate the effectiveness of radiation-protective materials. The HVL is defined as the thickness of a material required to reduce the intensity of incident X-ray photons by 50%, whereas the TVL represents the thickness needed to attenuate 90% of the incident radiation. Both parameters were determined from the linear attenuation coefficient (LAC) using Eqs. (3) and (4), respectively [46]. Lower HVL and TVL values indicate superior radiation shielding performance, as a thinner material is sufficient to achieve the desired level of X-ray attenuation [37, 47].

$$HVL = \ln(2)/\mu = 0.693/\mu \tag{3}$$

$$TVL = \ln(10)/\mu = 2.303/\mu \tag{4}$$

The variation of HVL and TVL with X-ray tube voltage for the TBZNW1-TBZNW4 glass samples is presented in Figures 3 & 4, while the corresponding numerical values are summarized in Table 1.

Table 1. *Calculated values of radiation shielding parameters of the WO_3-doped TBZNW glass system.*

Sample Code	WO_3 (mol%)	Peak Voltage (kVp)	LAC (cm^{-1})	MAC ($cm^2\ g^{-1}$)	HVL (cm)	TVL (cm)	MFP (cm)	Attenuation (%)	LET at 100 kVp (mm)
TBZNW1	5	75	21.68987	4.94976	0.03195	0.10613	0.04610	99.987	2.514
		100	15.59872	3.55973	0.04443	0.14758	0.06411	99.842	
		120	12.20462	2.78517	0.05678	0.18862	0.08194	99.358	
		140	10.07095	2.29826	0.06881	0.22858	0.09930	98.449	
TBZNW2	10	75	23.52658	5.09454	0.02946	0.09785	0.04251	99.993	2.784
		100	17.32026	3.75060	0.04001	0.13291	0.05774	99.921	
		120	13.81081	2.99065	0.05018	0.16668	0.07241	99.664	
		140	11.32111	2.45152	0.06121	0.20334	0.08833	99.063	
TBZNW3	15	75	25.60983	5.27277	0.02706	0.08989	0.03905	99.997	3.152
		100	19.75709	4.06776	0.03508	0.11652	0.05061	99.969	
		120	16.00276	3.29478	0.04331	0.14385	0.06249	99.857	
		140	13.27234	2.73262	0.05221	0.17344	0.07534	99.563	
TBZNW4	20	75	28.38071	5.56266	0.02442	0.08111	0.03524	99.999	3.560
		100	22.24693	4.36043	0.03115	0.10347	0.04495	99.990	
		120	18.31758	3.59027	0.03783	0.12567	0.05459	99.950	
		140	15.34601	3.00784	0.04516	0.15001	0.06516	99.829	

The results indicate that both HVL and TVL decrease progressively with increasing WO_3 concentration. This behaviour is primarily attributed to the enhancement in glass density and the corresponding increase in LAC following the incorporation of tungsten oxide [48, 49]. Materials possessing higher density and larger attenuation coefficients provide more effective interactions with incident X-ray photons, thereby requiring a smaller thickness to achieve the same degree of radiation attenuation. Consequently, lower HVL and TVL values reflect improved shielding efficiency [41].

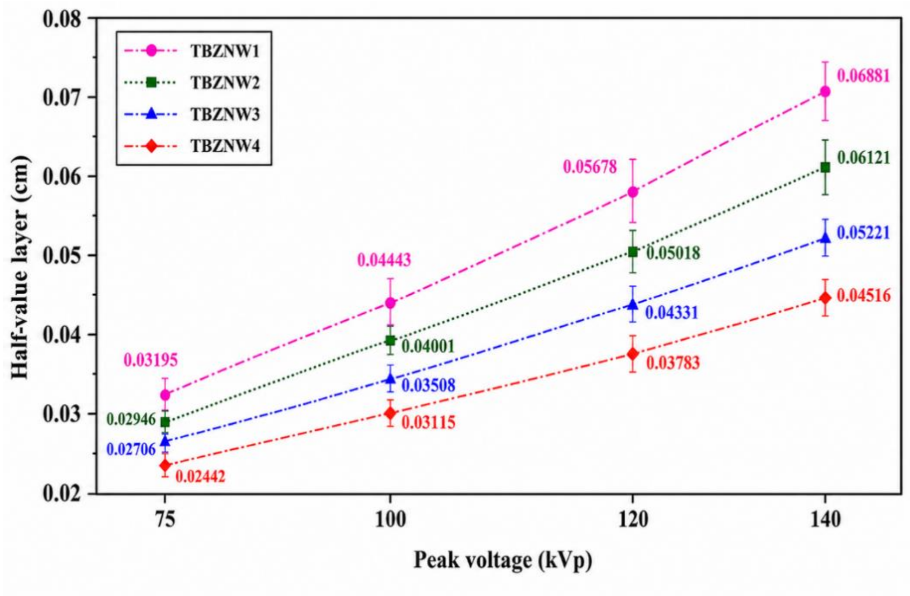

Figure 3. *Half-value layer (HVL) Vs X-ray tube voltage.*

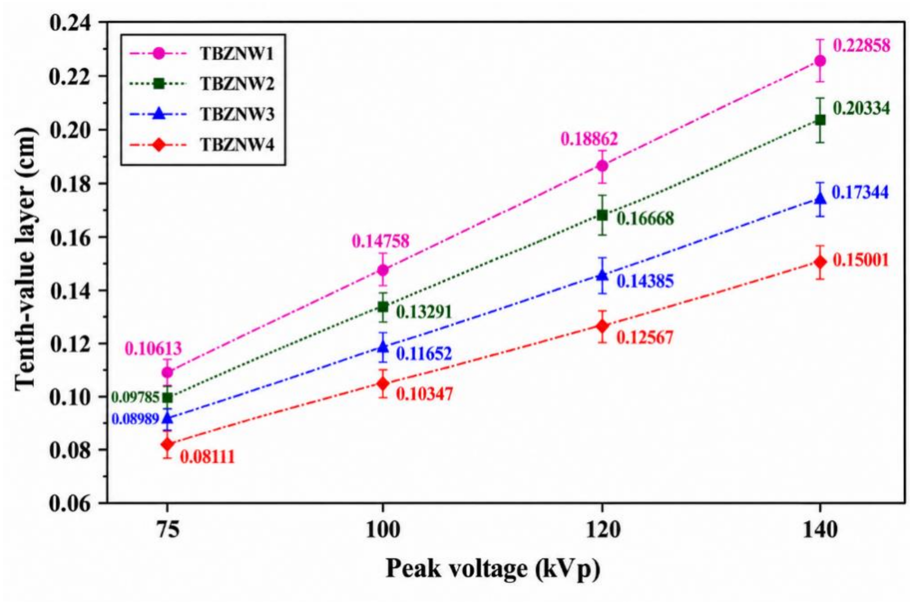

Figure 4. *Tenth-value layer (TVL) Vs X-ray tube voltage.*

In contrast, both HVL and TVL increase with increasing X-ray tube voltage [40, 43]. At higher photon energies, X-rays possess greater penetrating power, reducing the probability of interaction within the shielding material. As a result, a greater material thickness is required to attenuate the radiation, leading to higher HVL and TVL values. This trend is consistent with those reported for similar glass systems in previous studies [35, 37].

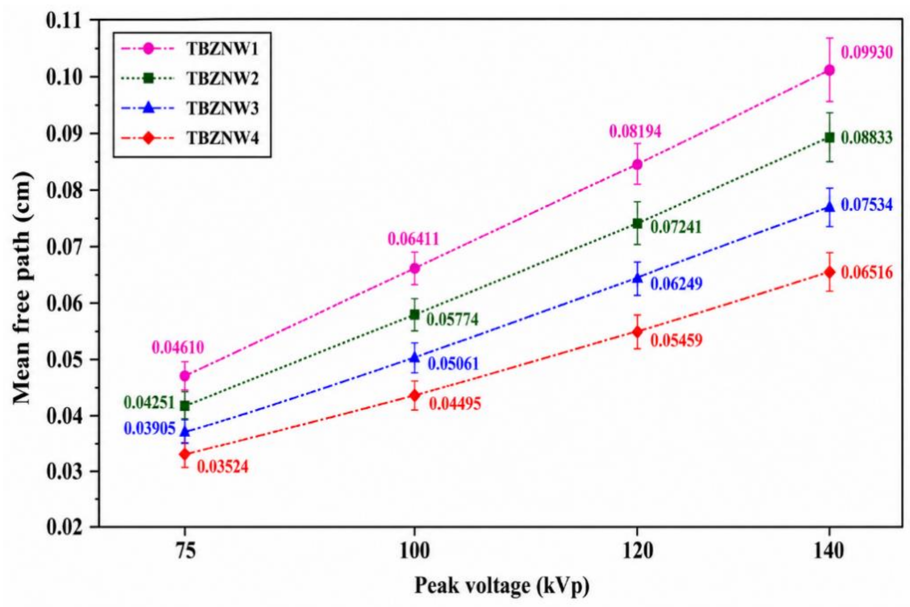

Figure 5. *Mean free path (MFP) Vs X-ray tube voltage.*

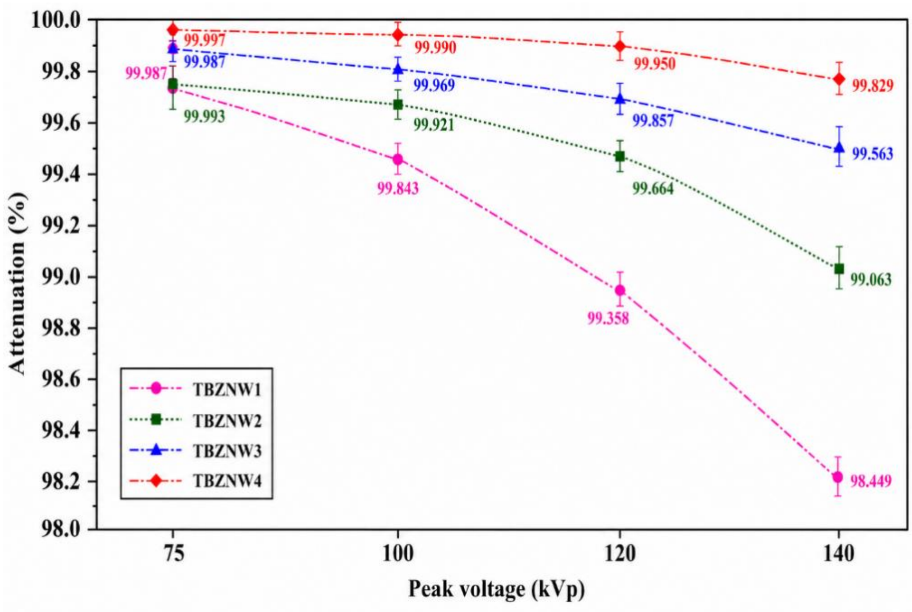

Figure 6. *Radiation shielding efficiency (Att%) Vs X-ray tube voltage.*

Among the investigated compositions, TBZNW4, containing the highest WO_3 concentration, exhibited the lowest HVL and TVL values, demonstrating its superior radiation attenuation capability. The enhanced shielding performance of this composition can be attributed to its higher density and improved photon interaction probability compared with the other glass samples. Furthermore, the developed TBZNW glass system exhibited lower HVL values than commercial window glass, commercial lead glass, and several previously reported lead-free glass systems, including BaO-ZnO-B_2O_3, BaO-Na_2O-ZnO-B_2O_3, and Gd_2O_3-La_2O_3-ZnO-B_2O_3-Sm_2O_3 glasses [40, 42]. These comparisons further confirm the excellent shielding performance of the present glass compositions.

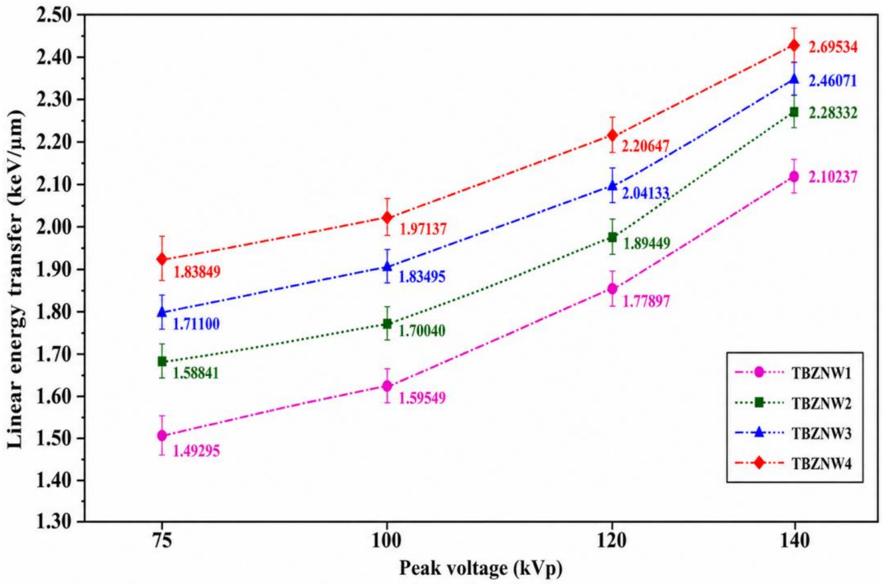

Figure 7. *Lead equivalent thickness (LET) Vs Peak Voltage.*

According to the National Council on Radiation Protection and Measurements (NCRP) Report 49, the HVL and TVL values of lead at 100 kVp are 0.27 mm and 0.88 mm, respectively [50]. Similar values have also been reported in the ANSI/HPS N43.3 standard published by the American National Standards Institute [51, 52]. The HVL and TVL values obtained for the present TBZNW glass system were found to be significantly lower than these standard lead values at the same photon energy, indicating superior attenuation capability. These results demonstrate that the developed WO_3-doped tellurite glass system possesses excellent X-ray shielding characteristics and can serve as an effective, environmentally friendly lead-free alternative for radiation protection in medical diagnostic applications.

4. Conclusion

A series of lead-free WO_3-doped boro-tellurite glasses with the composition (55 − x) TeO_2-$20B_2O_3$-15ZnO-$10Na_2CO_3$-xWO_3 (x = 5-20 mol%) were successfully synthesized using the conventional melt-quenching technique, and their X-ray shielding performance was experimentally investigated in the diagnostic energy range of 50-140 kVp. The results demonstrated that the incorporation of WO_3 significantly improved the radiation attenuation characteristics of the glass system. The linear attenuation coefficient (LAC) and mass attenuation coefficient (MAC) increased progressively with increasing WO_3 concentration, whereas the half-value layer (HVL), tenth-value layer (TVL), and mean free path (MFP) decreased, indicating enhanced shielding efficiency. The attenuation efficiency also increased with WO_3 content, while the lead equivalent thickness (LET) confirmed the suitability of the prepared glasses for practical radiation shielding applications. Among the investigated compositions, TBZNW4 (20 mol% WO_3) exhibited the best overall shielding performance because of its higher density and increased probability of photon interaction. The developed glass system also compared favourably with commercial shielding glasses and several previously reported lead-free glass compositions, demonstrating improved attenuation capability while avoiding the environmental and health concerns associated with lead-based materials. Overall, the experimental findings indicate that WO_3 incorporation is an effective approach for enhancing the X-ray shielding properties of boro-tellurite glasses. The excellent attenuation performance, combined with the inherent transparency, chemical stability, and lead-free composition of the developed glasses, makes them attractive candidates for radiation shielding windows, protective barriers, diagnostic imaging facilities, research laboratories, and other applications requiring safe and sustainable radiation protection. Future investigations may focus on evaluating their γ-ray shielding behaviour, long-term durability, mechanical performance, and large-scale fabrication to further expand their practical applications.

Abbreviations

LAC	Linear Attenuation Coefficient
MAC	Mass Attenuation Coefficient
HVL	Half-Value Layer
TVL	Tenth-Value Layer
MFP	Mean Free Path
LET	Lead Equivalent Thickness

Author Contributions

Shihabudheen VT: Conceptualization, Data curation, Formal Analysis, Investigation, Methodology, Writing – original draft, Writing – review & editing

Ghizal Firdous Ansari: Conceptualization, Formal Analysis, Project administration, Resources, Supervision, Validation, Writing – review & editing

Conflicts of Interest

The authors declare no conflicts of interest.

References

[1] A. Ali, et al., Influence of WO3 on gamma radiation shielding efficiency, physical and optical properties of newly developed Li2O-CaO-Bi2O3-B2O3 glasses, Radiat. Phys. Chem. 198 (2022) 110240.

[2] M. Samdani, et al., Gamma shielding performance of B2O3/BaO-based glassy system: synthesis and simulation study, Radiat. Phys. Chem. 214 (2024) 111301.

[3] M. Mhareb, et al., The impact of barium oxide on physical, structural, optical, and shielding features of sodium zinc borate glass, J. Non-Cryst. Solids 541 (2020) 120090.

[4] G. Almisned, et al., A promising glass type in electronic and laser applications: elastic moduli, mechanical, and photon transmission properties of WO3 reinforced ternary-tellurite glasses, Symmetry 15(3) (2023) 602.

[5] R. B. Malidarre, et al., Analysis of radiation shielding, physical and optical qualities of various rare earth dopants on barium tellurite glasses: a comparative study, Radiat. Phys. Chem. 207 (2023) 110823.

[6] A. S. Ali, et al., Unveiling the structural, optical, and electromagnetic attenuation characteristics of B2O3-SiO2-CaO-Bi2O3 glasses with varied WO3 content, Radiat. Phys. Chem. 212 (2023) 111089.

[7] N. J. AbuAlRoos, et al., Tungsten-based material as promising new lead-free gamma radiation shielding material in nuclear medicine, Phys. Med. 78 (2020) 48-57.

[8] Protection, N. C. o. R. and Measurements, NCRP Report, National Council on Radiation Protection and Measurements, 1990.

[9] A. Bijanu, et al., Metal-polymer composites for radiation protection: a review, J. Polym. Res. 28(10) (2021) 392.

[10] J. Valentin, The 2007 Recommendations of the International Commission on Radiological Protection, vol. 37, Elsevier Oxford, 2007.

[11] A. Aboalatta, et al., Experimental investigation of zinc sodium borate glass systems containing barium oxide for gamma radiation shielding applications, Nucl. Eng. Technol. 53(9) (2021) 3058-3067.

[12] A. Madbouly, E. Atta, Comparative study between lead oxide and lead nitrate polymer as gamma-radiation shielding materials, J. Environ. Protect. 7(2) (2016) 268.

[13] Y. Rammah, et al., The f-factor, neutron, gamma radiation and proton shielding competences of glasses with Pb or Pb/Bi heavy elements for nuclear protection applications, Ceram. Int. 46(17) (2020) 27163-27174.

[14] M. Sayyed, et al., Exploring Gamma radiation shielding: the role of BaO in borosilicate glasses, Silicon (2024) 1-10.

[15] S. Malekie, H. Shooli, M. A. Hosseini, Assessment of new composites containing polyamide-6 and lead monoxide as shields against ionizing photonic radiation based on computational and experimental methods, Sci. Rep. 12(1) (2022) 9259.

[16] V. Agrawal, et al., Green conversion of hazardous red mud into diagnostic X-ray shielding tiles, J. Hazard Mater. 424 (2022) 127507.

[17] M. Sayyed, G. Lakshminarayana, Structural, thermal, optical features and shielding parameters investigations of optical glasses for gamma radiation shielding and defense applications, J. Non-Cryst. Solids 487 (2018) 53-59.

[18] M. I. Sayyed, et al. "Impacts of BaO additions on structure, linear/nonlinear optical properties and radiation shielding competence of BaO–NiO–ZnO–B_2O_3 glasses," Optical Materials, 144 (2023) 114300. https://doi.org/10.1016/j.optmat.2023.11430R

[19] S. Ravangvong, et al., Effects of WO3 on radiation shielding properties of WO3-TeO2 binary tellurite glass system, Integrated Ferroelectrics Int. J. 222(1) (2022) 125-135.

[20] S. M. Ngaram, et al., Enhanced physical, optical and radiation shielding properties of tungsten modified potassium boro-tellurite glass systems: theoretical approach, Radiat. Phys. Chem. 226 (2025) 112355.

[21] R. Ruamnikhom, et al., Hazardous radiation protective glasses for medical and research laboratories, Heliyon 9(9) (2023) e19935.

[22] H. Tekin, et al., Transmission factors, mechanical, and gamma ray attenuation properties of barium-phosphate-tungsten glasses: incorporation impact of WO3, Optik 267 (2022) 169643.

[23] A. M. Babeer, et al., Impact of mixed heavy metal cations (Ba and Bi) on the structure, optical and ionizing radiation shielding parameters of Bi2O3-BaO-Fe2O3-SrO-B2O3 glass matrix, Ceram. Int. 50(11) (2024) 19245-19258.

[24] K. Boonin, et al., Effect of BaO on lead free zinc barium tellurite glass for radiation shielding materials in nuclear application, J. Non-Cryst. Solids 550 (2020) 120386.

[25] R. K. Sk, et al., Structural, thermal and X-ray photoelectron spectroscopic properties of boro-tellurite based quaternary glass system, Opt. Mater. 156 (2024) 115989.

[26] B. B. Solak, et al., Exploring the radiation shielding properties of B2O3-PbO-TeO2- CeO2-WO3 glasses: a comprehensive study on structural, mechanical, gamma, and neutron attenuation characteristics, Mater. Chem. Phys. 312 (2024) 128672.

[27] M. Sayyed, et al., Effect of TeO2 addition on the gamma radiation shielding competence and mechanical properties of boro-

tellurite glass: an experimental approach, J. Mater. Res. Technol. 18 (2022) 1017-1027.

[28] S. Biradar, et al., Comprehensive investigation of borate-based glasses doped with BaO: an assessment of physical, structural, thermal, optical, and radiation shielding properties, Opt. Mater. 150 (2024) 115176.

[29] M. Sayyed, et al., The combination of high optical transparency and radiation shielding effectiveness of zinc sodium borate glasses by tungsten oxide additions, J. Alloys Compd. 904 (2022) 164037.

[30] S. Ravangvong, et al., Behaviors of TeO2-B2O3-WO3 glass system for ionizing radiation shielding performance: photon, protons and alpha particles, Mater. Today Proc. 65 (2022) 2269-2276.

[31] M. Elsafi, et al., Experimental investigation of the radiation shielding performance of a newly developed silicon-epoxy resin doped with WO3 micro/ nanoparticles, Silicon 16(13) (2024) 5439-5446.

[32] W. Cheewasukhanont, et al., High density of tungsten gadolinium borate glasses for radiation shielding material: effect of WO3 concentration, Radiat. Phys. Chem. 192 (2022) 109926.

[33] V. Zanganeh, Effect of WO3 addition on mechanical, structural, optical, and radiation shielding properties of lead boro phosphate glasses system using Monte Carlo simulation, Optik 269 (2022) 169900.

[34] A. H. Hammad, A. Abdelghany, G. Rabie, Extensive research into the structure, elasticity, optical, and radiation-shielding properties of zinc phosphate glasses doped with tungsten ions, Appl. Phys. A 130(4) (2024) 229.

[35] M. K. Hamad, Effect of WO3 on structural, optical, mechanical, and ionizing radiation shielding properties of borate-tellurite glass network, Ceram. Int. 51(8) (2025) 9763-9771.

[36] Y. S. Itas, et al., Studies of gamma ray shielding properties of lead-free tungsten- borate-tellurite glasses (x WO3-20B2O3-(80 x) TeO2);(x= 10, 15, 20 and 25), J. Electron. Mater. 53(9) (2024) 5696-5705.

[37] H. A. Esawii, et al., High impact tungsten-doped borosilicate glass composite for gamma and neutron transparent radiation shielding, Prog. Nucl. Energy 150 (2022) 104321.

[38] S. R. Karim, et al., X-ray attenuation performance of a newly synthesized tellurium based lead-free radiation shielding glass system, Radiat. Phys. Chem. (2023) 111477.

[39] S. Kaewjaeng, et al., Fabrication luminescence and radiation shielding properties of Gd2O3-La2O3-ZnO-B2O3-Sm2O3 glasses, Radiat. Phys. Chem. 202 (2023) 110537.

[40] A. H. Almuqrin, et al., Physical, optical and mechanical properties of BaO-WO3- P2O5 (BWP) glass system for radiation shielding, Opt. Quant. Electron. 56(6) (2024) 914.

[41] S. Sarachai, et al., Radiation shielding properties of BaO-ZnO-B2o3 glass for X- Ray room, Key Eng. Mater. 766 (2018) 88-93.

[42] S. Kaewjaeng, et al., X-ray radiation shielding of CeO2 doped borosilicate glasses and their luminescence characteristics, Radiat. Phys. Chem. 191 (2022) 109825.

[43] S. Mukamil, et al., Lead-borate glass system doped with Sm3+ ions for the X-ray shielding applications, Results Phys. 43 (2022) 106121.

[44] M. Ghaseminejad, L. Gholamzadeh, F. Ostovari, Investigation of x-ray attenuation property of modification PbO with graphene in epoxy polymer, Mater. Res. Express 8(3) (2021) 35008.

[45] A. Henaish, et al., Spectral, electrical, magnetic and radiation shielding studies of Mg-doped ni-cu-zn nanoferrites, J. Mater. Sci. Mater. Electron. 31 (2020) 20210-20222.

[46] M. Rashad, et al., Physical and nuclear shielding properties of newly synthesized magnesium oxide and zinc oxide nanoparticles, Nucl. Eng. Technol. 52(9) (2020) 2078-2084.

[47] N. A. Alsaif, et al., Influence of WO3 replacement for CaO on physical, optical, and γ-ray protection properties of borotellurite glasses: a comparative study, Ceram. Int. 50 (2024) 32687-32698.

[48] M. Zhukovsky, et al., Dielectric, structural, optical and radiation shielding properties of newly synthesized CaO-SiO2-Na2O-Al2O3 glasses: experimental and theoretical investigations on impact of Tungsten (III) oxide, Appl. Phys. A 128(3) (2022) 205.

[49] National Council on Radiation Protection and Measurements (NCRP), Structural shielding design and evaluation for medical use of x rays and gamma rays of energies up to 10 MeV, Bethesda: NCRP (1976) 49.

[50] American National Standards Institute (ANSI), ANSI/HPS N43.3. Installations Using Non-medical x-ray and Sealed gamma-ray Sources, Energies up to 10 Mev, ANSI, 2008.

[51] N. H. Kwon, et al., Review of shielding evaluation methodology for facilities using kV energy radiation generating devices based on the NCRP-49 report, Progress in Medical Physics 33(4) (2022) 53-62.

[52] S. A. Issa, et al., Structure, optical, and radiation shielding properties of PVA-BaTiO3 nanocomposite films: an experimental investigation, Radiat. Phys. Chem. 180 (2021) 109281.